Journal of Thermal Analysis and Calorimetry (2018) 134:1481–1492
https://doi.org/10.1007/s10973-018-7618-8

An experimental investigation of hydration mechanism of the binary cementitious pastes containing MgO and Al_2O_3 micro-powders

Dominika Madej[1] · Ryszard Prorok[1] · Klaudia Wiśniewska[1]

Received: 26 March 2018 / Accepted: 29 July 2018 / Published online: 16 August 2018
© The Author(s) 2018

Abstract
The reactivity of the binary mixtures of reactive magnesia and hydratable alumina micro-powders with various compositions was investigated by calorimetric method, X-ray diffraction, simultaneous DSC–TGA with thermal evolved gas analysis–mass spectrometry and scanning electron microscope observations. The effect of the MgO/Al_2O_3 molar ratio (2:1, 1:1 and 1:2) and temperature on the hydration behavior of pastes has been explored using the TAM Air isothermal calorimetry system at 25 and 50 °C. Some structural aspects of a M–A–H ($M \equiv MgO$, $A \equiv Al_2O_3$, $H \equiv H_2O$) binding phase formed upon the hydration of $MgO–Al_2O_3$ micro-powders at different curing time have been explored. The main hydrate considered to be important in this system is hydrotalcite $Mg_6Al_2CO_3(OH)_{16}{\cdot}4H_2O$ formed via the isomorphous substitution of Mg^{2+} ions by trivalent Al^{3+} one in the brucite-like sheet. This was expressed as a systematic shift of the peak at 2-theta value corresponding to the (003) reflection. Since both hydrotalcite and brucite are identified in the hydrating samples, the thermal stability of hydroxyls in these hydration products can be placed in the decreasing order as follows: (Mg2Al)–OH-hydrotalcite group > (Mg3)–OH-brucite group > (Mg3)–OH-hydrotalcite group.

Keywords Heat flow calorimetry · Thermal analysis · Time and temperature-dependent hydration mechanism · Hydrotalcite · Structural properties

Introduction

Magnesia (MgO) is widely used in the production of refractory materials due to its ultra-high melting point and ability to form the binding system based on M–S–H ($M \equiv MgO$, $S \equiv SiO_2$, $H \equiv H_2O$) phase under moist conditions and in the presence of, for example, silica fume [1–4]. Magnesium oxide with high chemical activity can be obtained by optimizing the technological parameters including calcination temperature and soaking time. The most reactive MgO produced at the lowest calcination temperature with the highest surface area and the smallest crystallite size is required for the latest application [5–8]. In connection with these subjects, due to the excellent high temperature properties of α-alumina, calcined aluminas are also used in many refractory applications, in both monolithic and shaped products [9–11]. Processing of simple metal-oxides, i.e., fine nano- and micro-powders of both MgO and Al_2O_3 in unshaped refractory materials (castables) technology, is now up-to-date trend of corundum-spinel castables, mainly cement-bonded refractory castable and no-cement-content (NCC) castables [10, 12–15]. Some literature reports concern a combination of $MgO–Al_2O_3$ oxide system as a promising state-of-the-art binding system based on M–A–H ($A \equiv Al_2O_3$) phase designed for the calcia-free refractory castables [10, 15, 16]. In our recent paper [15], it has been shown that the powder fineness and particle size distribution result in a size-dependent hydration mechanism and kinetics for MgO and Al_2O_3, and also determine cementitious (hydraulic) activities. In situ reactions based on the formation of hydrotalcite-like phases inside the refractory MgO-bonded alumina castables were recently evaluated by Santos Jr. et al. [12] and Ye et al. [10]. Hydrotalcite, a natural mineral of chemical formula $Mg_6Al_2(OH)_{16}(CO_3){\cdot}4H_2O$, is a close mineral belonging to the layered

✉ Dominika Madej
dmadej@agh.edu.pl

[1] Faculty of Materials Science and Ceramics, AGH University of Science and Technology, Mickiewicza 30 Av, 30-059 Krakow, Poland

double hydroxide family of anionic clays [17–21]. It was proved that the hydrotalcite-like phases might enhance the explosion resistance of Al_2O_3–MgO refractory castables, since these compounds exhibit crystalline lamellas separated by water molecules [12].

Based on these aspects, this paper firstly evaluates the influence of both MgO/Al_2O_3 molar ratio and curing time on the kinetics of water release from binder samples, and secondly discusses some structural aspects of a M–A–H binding phase formed upon the hydration of $MgO–Al_2O_3$ micro-powders. The main objective of this study was to demonstrate an alternative route to elaborate the calcia-free hydraulic binder systems designed for refractory corundum castables with in situ spinel formation.

Experimental

Materials

The raw materials were high-purity hydratable alumina NABALOX NO 115 TC, d_{50} = 3.5–5.0 µm, 99.5% Al_2O_3, α-Al_2O_3-content approx. 98.0%) from NABALTEC and analytical reagent quality magnesium oxide (d_{50} = 10 µm, 98% MgO) from Acros Organics. All cementitious pastes were prepared using distilled water.

Preparation

A novel magnesia–alumina-based binder for in situ spinel-bonded refractory castables was prepared by mixing MgO and Al_2O_3 reactive micro-powders with MgO/Al_2O_3 molar ratios of 1:0, 2:1 and 1:2. Dry raw materials were weighted and pre-homogenized together. The water–solid material ratio (abbreviated w/s) was used as a basis for sample mixture proportioning. The cementitious pastes MA 1:1, MA 2:1 and MA 1:2 were prepared with w/s = 0.7, and then, all neat pastes were mixed by hand in the glass beaker with a metal spatula until the powders and water were uniformly distributed (approximately 5 min mix time). Three cementitious paste samples were placed in sealed polyethylene bag and cured up to 2 years in a climatic chamber. The sealed/saturated curing conditions (relative humidity ∼ 96%, temperature ∼ 50 °C) were maintained.

Characterization

Proof of crystalline mineral phases in hydrated cementitious pastes was performed by X-ray detection (XRD). The X-ray analysis was performed by a X'Pert Pro PANalytical X-ray diffractometer using the following device parameters: CuKα radiation, stepsize 0.02° 2-theta, start: 5.00°, end 70.00°, temp. 25 °C. Thermal decomposition data for hydrated compounds were obtained using simultaneous TG–DSC–EGA method (NETZSCH STA 449 F5 Jupiter) at a heating rate of 10 °C min^{-1} under a flow of air (25 mL min^{-1}) with alumina as a standard substance. The TG–DSC analyses were performed using a sample mass of 25 mg in alumina crucibles. The phase distribution and microstructural changes of the M–A–H hardened pastes were analyzed using scanning electron microscopy (SEM, Nova Nano SEM 200, FEI).

The samples for XRD and TG–DSC–EGA investigations were obtained by grinding the hardened pastes with acetone. Thus, the hydration reactions were stopped at appropriate time intervals, i.e., 140 days, 255 days and 2 years.

Hydration heat evolution of the blended pastes containing MgO and Al_2O_3 reactive micro-powders with MgO/Al_2O_3 molar ratios of 1:0, 2:1 and 1:2 was determined with a TAM Air microcalorimeter (TA Instruments) at 25 °C and 50 °C by integrating the continuous heat flow signal during the 72-h and 16-h hydration processes, respectively. An in situ mixing procedure using admix ampoule was applied for this purpose [16]. In all cases, two grams specimen of dry homogenized mixture was poured into a glass vial. Water was weighed into mounted syringes. Admix ampoule was introduced into the calorimeter prior mixing, thus equilibrating to isothermal environment. Mixing step was done after equilibration inside the calorimeter to enable the quantitative access to the early-age hydration peak. A second glass vial containing sand was used as an inert reference in the twin channel of calorimeter to ensure best stability of the baseline before mixing step and after experiment. This reference materials provide the same heat capacity than the mass of binder paste.

Results and discussion

X-ray diffraction characterization of Mg–Al cementitious matrices

All results of XRD on samples are presented in Figs. 1–4 and listed in Tables 1–4. The X-ray diffraction (XRD) method was applied to analyze whether MgO/Al_2O_3 affects the hydration progress of Mg–Al cementitious matrices prepared with the reactive micro-sized alumina and reagent grade magnesium oxide. Figures 1–3 present diffractograms of the Mg–Al cementitious matrices concerning phase evolution over the curing time. The multiphase composition of the Mg–Al cementitious pastes becomes evident at 140, 255 days and 2 years of curing time. Among the crystalline phases, α-Al_2O_3 and $Mg(OH)_2$ phases are the most easily recognizable. The magnesium oxide particles were fully hydrated to magnesium hydroxide at every

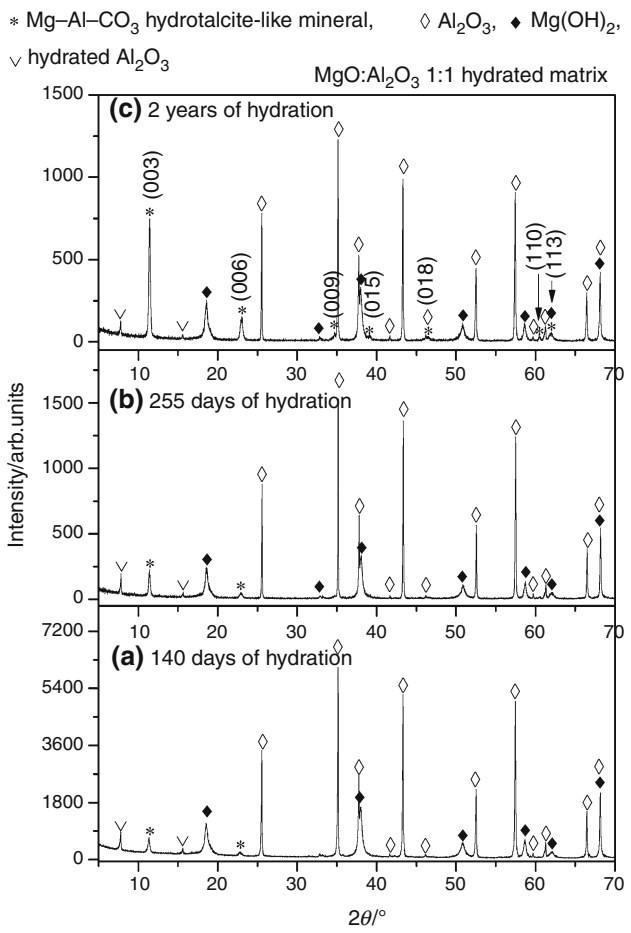

Fig. 1 X-ray diffraction patterns of the MgO/Al_2O_3 1:1 hydrated matrix (w/s = 0.7) after 140 days **a** 255 days, **b** and 2 years, **c** of moist curing at 50 °C

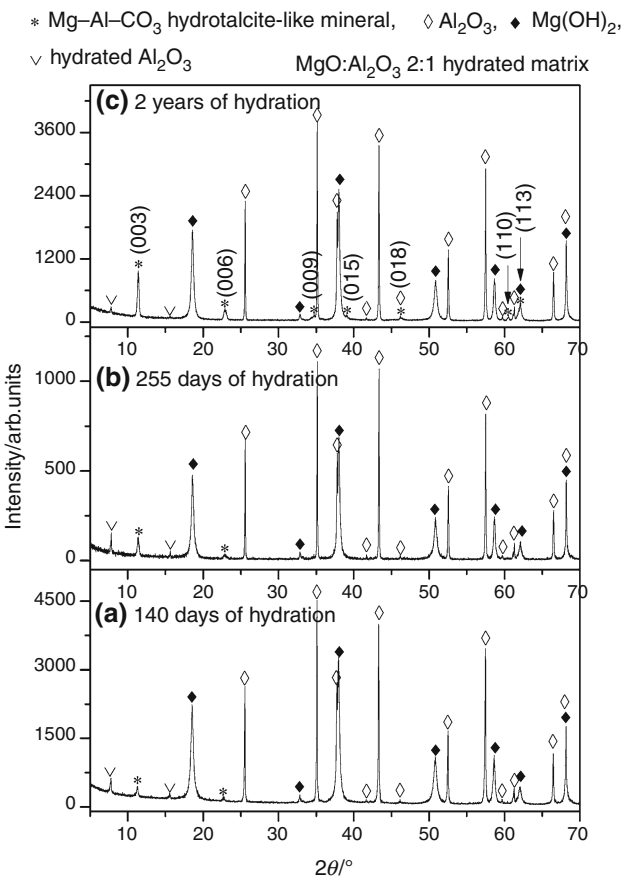

Fig. 2 X-ray diffraction patterns of the MgO/Al_2O_3 2:1 hydrated matrix (w/s = 0.7) after 140 days **a** 255 days, **b** and 2 years, **c** of moist curing at 50 °C

curing stage, and no traces of MgO were noticed in the Mg–Al cementitious samples.

In general respect, the cementitious paste is a very complex composite, where many crystalline phases coexist surrounded by an amorphous product, the M–A–H gel. The crystalline peaks do not show clear increase in peak width, but only a decrease in intensities of each diffraction peak with curing time from the first 140 days to 255 days. This indicates that the transition from crystal to amorphous was a direct transformation and can be best modeled as a mixture of amorphous in character and crystalline materials (Figs. 1–3a, b). Then, M–A–H structure has transformed from amorphous to crystalline during the curing period from 255 days to 2 years (Figs. 1–3b, c). As the time progressively increases, the formation of magnesium–aluminate–hydrate (M–A–H), a key product of hydrated cementitious pastes, takes place. For an example, the variation of the diffraction peak relative intensity of $Mg(OH)_2$ versus the hydration time in the MAH sample is presented in Table 1. The relative peaks intensity of brucite is decreased up to 255 days of hydration, and it can be deduced that the decreased crystallinity of $Mg(OH)_2$ is resulted from consumption of $Mg(OH)_2$ against hydration time. Unexpected increase in intensity of XRD peaks of $Mg(OH)_2$ between 255 days and 2 years of hydration is rather difficult to explain. With these results, it can be supposed that an increase in intensity of XRD peaks of Mg(OH)2 could be regarded as the dissolution–recrystallization–redissolution–recrystallization of magnesium hydroxide that proceeded within continuous moist curing of pastes. In fact, it can also be assumed that the measured powder sample exhibits preferred orientation; thus, the relative intensity between peaks changes, as the intensity ratios of I_{001}/I_{101}, I_{001}/I_{102}, I_{001}/I_{110} are presented in Table 2.

The X-ray powder diffraction patterns of the MA 1:1, MA 2:1 and MA 1:2 cementitious matrices (Figs. 1–3) exhibit some of the typical diffraction peaks at about 7.69, 3.88, 2.58 and 1.53 Å generally assigned to (003), (006), (009) and (110) planes of $Mg_6Al_2CO_3(OH)16{\cdot}4H_2O$ (Hydrotalcite, PDF-00-014-0191) [22]. There is an evidence in

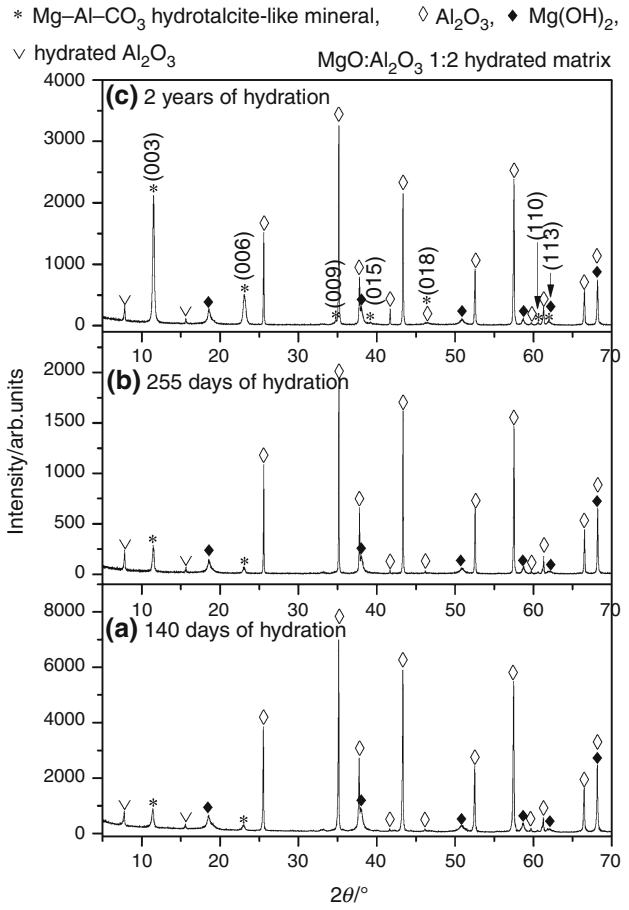

Fig. 3 X-ray diffraction patterns of the MgO/Al_2O_3 1:2 hydrated matrix (w/s = 0.7) after 140 days **a** 255 days, **b** and 2 years, **c** of moist curing at 50 °C

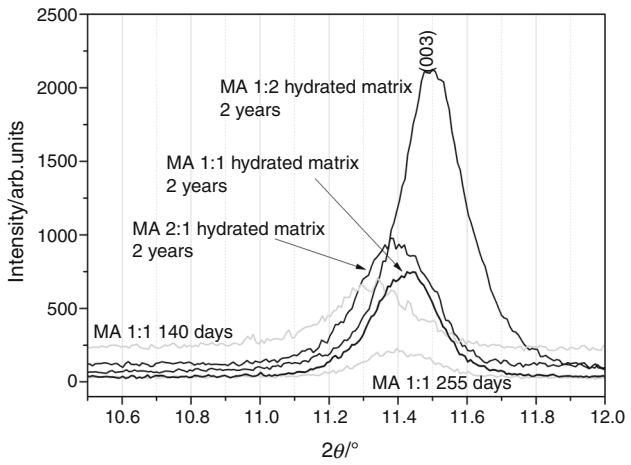

Fig. 4 Positions of the diffraction peaks assigned to (003) plane of $Mg_6Al_2CO_3(OH)_{16}{\cdot}4H_2O$ (Reference code: 00-014-0191 [22]) in the MgO/Al_2O_3 cementitious matrices with different composition (MgO/Al_2O_3 molar ratios of 2:1, 1:1 and 1:2) cured for 2 years. Positions changes versus time for MA 1:1 hydrated matrix are marked in gray

Table 1 The relative intensity (in %) of the diffraction peak at about d = 2.36373 Å assigned to (101) plane of $Mg(OH)_2$ (Reference code: 00-007-0239 [22]) in the MgO/Al_2O_3 hydrated matrices versus hydration time

Hydration time	MgO/Al_2O_3 molar ratio		
	2:1	1:1	1:2
140 days	74.18	25.08	10.82
255 days	60.23	20.33	9.02
2 years	65.01	25.70	8.82

Table 2 The intensity ratios between some diffraction planes of $Mg(OH)_2$ extracted from XRD patterns

Hydration time	I_{001}/I_{101}	I_{001}/I_{102}	I_{001}/I_{110}
MgO/Al_2O_3 molar ratio of 2:1			
140 days	0.66	2.13	1.98
255 days	0.66	2.08	1.96
2 years	0.68	2.20	2.16
MgO/Al_2O_3 molar ratio of 1:1			
140 days	0.66	2.12	1.80
255 days	0.70	2.36	1.87
2 years	0.67	2.38	2.16
MgO/Al_2O_3 molar ratio of 1:2			
140 days	0.60	2.15	1.55
255 days	0.70	2.40	1.84
2 years	0.80	3.05	2.64

the gradual increase in XRD peak intensities corresponding to an increase in both crystallinity and hydrotalcite content along with increase in the curing time. As the hydration proceeded over time, the intensity peak corresponding to the strongest peak from the crystallographic plane (003) of the $Mg_6Al_2CO_3(OH)_{16}{\cdot}4H_2O$ gradually increased (Table 3). Perhaps, the most important observation regarding the mechanisms of the products formed during hydration is that the alumina can significantly enhance the formation of the M–A–H phases. This is clearly seen in the pastes prepared using mixed oxides with stoichiometric composition and with an excess of Al_2O_3 with respect to the stoichiometric value of MA 1:1, i.e., in both MA 1:1 and MA 1:2 samples.

Hydrotalcite $Mg_6Al_2CO_3(OH)_{16}{\cdot}4H_2O$ crystallizes with hexagonal symmetry crystal structure. The lattice parameters both a (= $2d_{110}$) and c (= $3d_{003}$), were determined from powder X-ray diffraction data. Details of the procedure are presented elsewhere [15]. Table 4 lists the crystal parameters and the calculated sizes of the hydrotalcite-like compound within the $MgO–Al_2O_3$ cementitious matrices with MgO/Al_2O_3 molar ratios of 1:1, 2:1 and 1:2 cured for 2 years. The effect of Mg/Al molar ratios in the

Table 3 The relative intensity (in %) of the diffraction peak at about d = 7.690 Å assigned to (003) plane of $Mg_6Al_2CO_3(OH)_{16}{\cdot}4H_2O$ (Reference code: 00-014-0191 [22]) in the MgO/Al_2O_3 hydrated matrices versus hydration time

Hydration time	MgO/Al_2O_3 molar ratio		
	1:1	2:1	1:2
140 days	7.46	7.52	9.04
255 days	12.33	9.09	13.53
2 years	59.80	22.51	65.89

Table 4 XRD data and structural parameters of hydrotalcite-like compound within the $MgO–Al_2O_3$ cementitious matrices with different composition (MgO/Al_2O_3 molar ratios) cured for 2 years

Structural parameter	MA 2:1	MA 1:1	MA 1:2
d_{003}/nm	0.7768	0.7749	0.7693
d_{110}/nm	0.1530	0.1530	0.1528
β for [003]/°	0.2502	0.2223	0.2271
β for [110]/°	0.2410	0.1536	0.2320
Lattice parameter a/nm (= $2d_{110}$)	0.3060	0.3060	0.3056
Lattice parameter c/nm (= $3d_{003}$)	2.3304	2.3247	2.3079
Crystallite size in the direction a/nm	37.77	59.25	39.25
Crystallite size in the direction c/nm	31.58	35.54	34.79

cementitious pastes on the structural properties of hydrotalcite is evident. The calculated value of the lattice parameter c, corresponding to the thickness of the brucite-like layers and the interlayer space, decreases in the series of MgO/Al_2O_3 molar ratios of 2:1, 1:1 and 1:2. It suggests that hydrotalcite formed in the Mg–Al cementitious matrix was enriched with a larger proportion of the smaller, trivalent Al ions. As it can be also observed in Fig. 4, the position of 2-theta is shifted for (003) plane of $Mg_6Al_2CO_3(OH)_{16}{\cdot}4H_2O$ toward higher 2 theta value. Thus, the isomorphic substitution of the Mg^{2+} ions by the smaller Al^{3+} ions is determined by both chemical composition (MgO/Al_2O_3 molar ratio (Mg/Al ratio)) of the cementitious paste and curing time. The light grey lines represent the observed data for MA 1:1 matrix hydrated for 255 days and 2 years.

Thermal analysis of Mg–Al cementitious matrices

Simultaneous DSC–TG–EGA measurements show several decomposition stages of the Mg–Al cementitious matrices with different composition (MgO/Al_2O_3 molar ratios of 2:1, 1:1 and 1:2) after curing time of 2 years (Figs. 5–7). The consumption of free water for cementitious materials hydration, especially as MgO/Al_2O_3 molar ratio dependent, can be clearly seen. The progress of hydration processes produces hydrates; thus, the highest loss of mass due to the evaporation of the water chemically bonded to Mg–Al phases was achieved after 2 years of moist curing (Table 5). According to thermogravimetric analysis results displayed as TG curves and the values presented in Table 5, the total mass loss due to decomposition of the hardened binder pastes within the temperature range − 35 °C to 1050 °C was 19.85, 16.72 and 11.14% of the initial mass of the MA 2:1, MA 1:1 and MA 1:2 samples, respectively. The MA 2:1 cementitious material is more susceptible to hydration than its MA 1:1 and MA 1:2 counterparts, owing to its higher magnesia content.

The high mass loss up to 420 °C is associated with endothermic peaks in the DSC curves and was due to the loss of three kinds of water (surface, interlayer and structural water) from both hydrotalcite and brucite. Based on

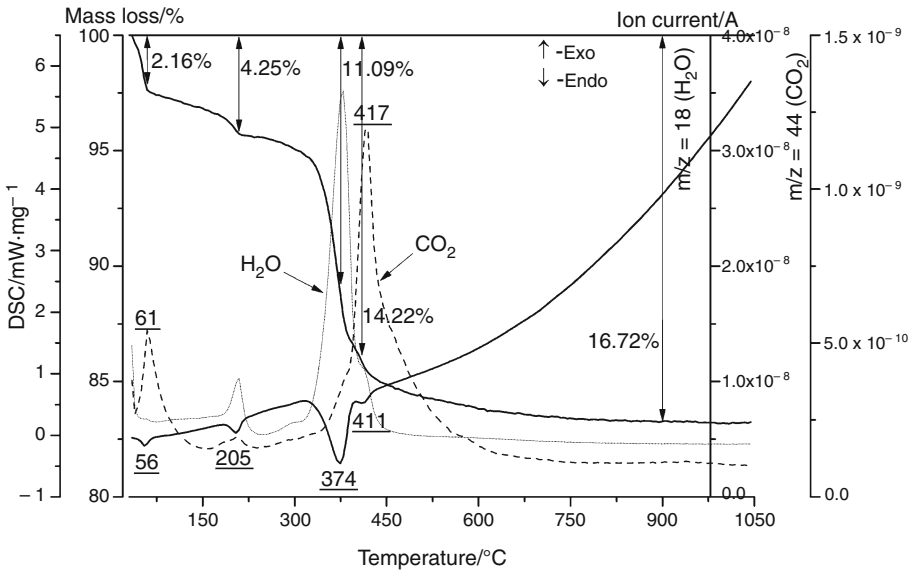

Fig. 5 Simultaneous DSC–TG curves (solid lines) of Mg–Al cementitious matrix with MgO/Al_2O_3 molar ratio of 1:1 measured in air at flow rate 50 mL min^{-1} (heating rate 10 °C min^{-1}, initial mass 25 mg). EGA–gas evolution curves for representative mass spectroscopic ion fragments of H_2O (dot line) and CO_2 (dash line) vapors

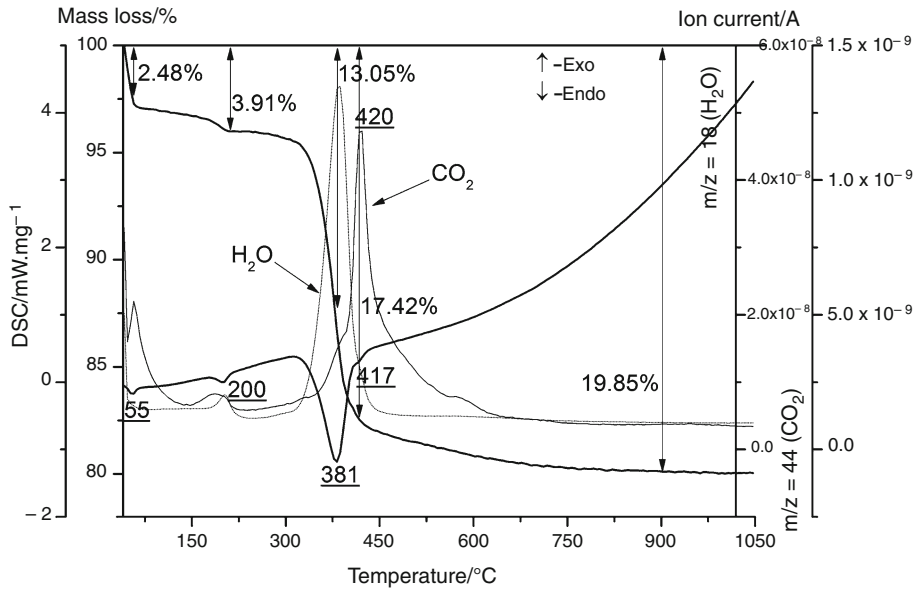

Fig. 6 Simultaneous DSC–TG curves (solid lines) of Mg–Al cementitious matrix with MgO/Al_2O_3 molar ratio of 2:1 measured in air at flow rate 50 mL min^{-1} (heating rate 10 °C min^{-1}, initial mass 25 mg). EGA–gas evolution curves for representative mass spectroscopic ion fragments of H_2O (dot line) and CO_2 (dash line) vapors

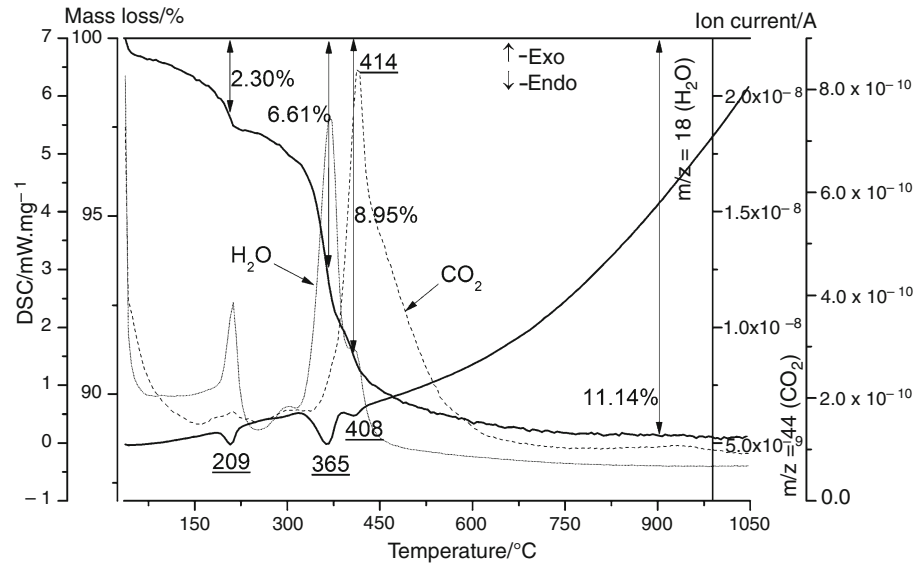

Fig. 7 Simultaneous DSC–TG curves (solid lines) of Mg–Al cementitious matrix with MgO/Al_2O_3 molar ratio of 1:2 measured in air at flow rate 50 mL min^{-1} (heating rate 10 °C min^{-1}, initial mass 25 mg). EGA–gas evolution curves for representative mass spectroscopic ion fragments of H_2O (dot line) and CO_2 (dash line) vapors

data from the literature, it can be generally agreed that the removal of physically adsorbed and interlayer water molecules (dehydration, removal of H_2O) occurs below 300 °C, but both dehydroxylation of hydroxide layers (elimination of OH^- groups) and loss of exchange anions CO_3^{2-} and OH^-) occur in the temperature range from 300 to 500 °C [23–27]. In these studies, the gaseous products evolved from the samples were also analyzed. Evolution of both H_2O (m/z = 18) and CO_2 (m/z = 44) shows parallel run to the DSC curves having local maximums at the same temperature values. The endothermic dehydration and decarbonization peaks are more sensitively detected by the MS than DSC curves, and the characteristic peaks of evolution of H_2O and CO_2 are clearly visible in all cementitious matrices. The results of MS are presented as a plot of the total ion current against the temperature (H_2O—dot line—and CO_2—dash line).

We have thus assigned the events at around 381, 374 and 365 °C to dehydroxylation of (Mg3)–OH-brucite sites and (Mg3)–OH-hydrotalcite sites, since both $Mg(OH)_2$ and $Mg_6Al_2CO_3(OH)_{16}{\cdot}4H_2O$ were detected by XRD in the 2-year hydrated MA 2:1, MA 1:1 and MA 1:2 samples. This assignment predicts the lower thermal stability of (Mg3)–OH-hydrotalcite sites than that of OH in $Mg(OH)_2$. Also note that the Al^{3+} ion stabilizes (Mg_2Al)–OH group [15, 28] and increases its thermal stability to 417, 411 and 408 °C in the 2-year hydrated MA 2:1, MA 1:1 and MA 1:2 samples, respectively.

Table 5 Thermoanalytical data for the $MgO–Al_2O_3$ cementitious matrices cured at 50 °C for 2 years

Samples	DSC peak temperature/°C	TG data/%	DTG data/%
MA 2:1	55	2.48	2.48
	200	3.91	1.43
	381	13.05	9.14
	417	17.42	4.37
	Total mass loss at 900 °C from TG data/%	19.85	2.43
MA 1:1	56	2.16	2.16
	205	4.25	2.09
	374	11.09	6.84
	411	14.22	3.13
	Total mass loss at 900 °C from TG data/%	16.72	2.50
MA 1:2	209	2.30	2.30
	365	6.61	4.31
	408	8.95	2.34
	Total mass loss at 900 °C from TG data/%	11.14	2.19

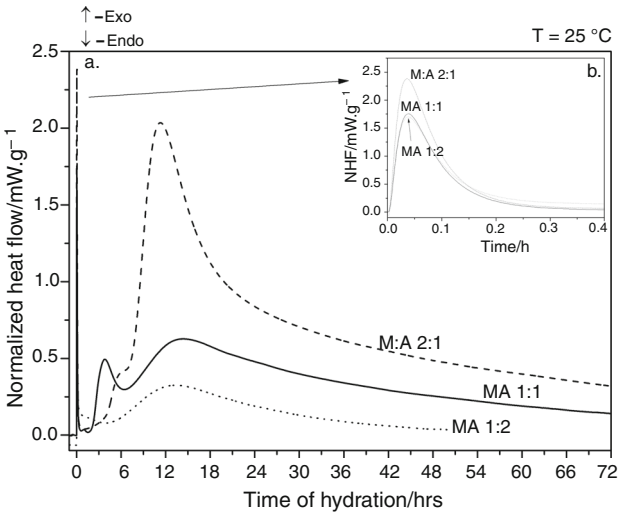

Fig. 8 Heat flow curves of reactive magnesia–hydratable alumina pastes hydrated at 25 °C for w/s = 0.7, normalized to mass of dry mixtures (with in situ mixing). MgO/Al_2O_3 molar ratio (M/A for short) of 1:1, 2:1 and 1:2

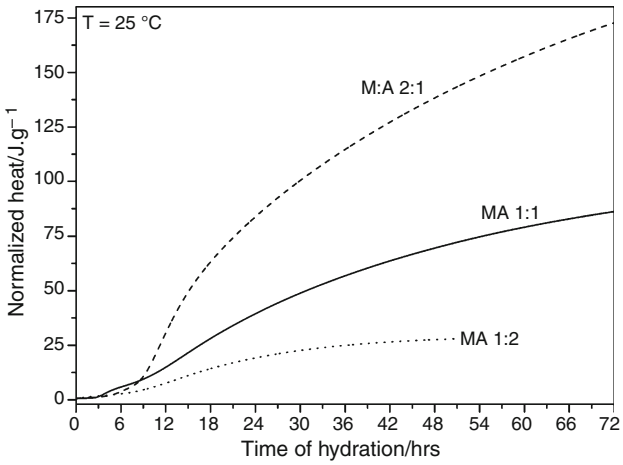

Fig. 9 Cumulative heat of reactive magnesia–hydratable alumina pastes hydrated at 25 °C for w/s = 0.7. MgO/Al_2O_3 molar ratio (M/A for short) of 1:1, 2:1 and 1:2

Calorimetric studies of reactive magnesia–hydratable alumina hydrating mixtures

The heat of hydration was measured for the mixtures of reagent oxides MgO and Al_2O_3 (MgO/Al_2O_3 1:1, 2:1 and 1:2 in molar ratios) whose particle size distribution known as the median diameter or the medium value of the particle size distribution was about 10 μm. The isothermal heat flow calorimetry measurement taken at two temperatures (25 °C and 50 °C) was a useful tool for both studying and assessing the hydration behavior of new alternative binders for corundum castable compositions. The heat flow curves for the MA 1:1, MA 2:1 and MA 1:2 hydrating special cementitious mixtures prepared with a water/solid ratio of 0.7 at 25 °C and 50 °C are presented in Figs. 8 and 10, respectively. The accelerating effect of temperature was clearly visible from calorimetric curves plotting the rates of heat evolution in W g^{-1} by all hydrating MA pastes as a function of time when reacted with water for 72 h and 16 h at temperatures from 25° to 50 °C. The exothermic heat effects observed in the microcalorimeter at 25 °C (Fig. 8) were shortened to a few hours for the measurement temperature of 50 °C (Fig. 10). The calorimetric curves measured at 25 °C exhibit three major details (Fig. 8). The first of these is intense heat evolution peak which occurs directly after mixing dry material with water (a mixing peak). The heat effect in the first 20 min is attributable to both the heat of initial wetting of the powder with the

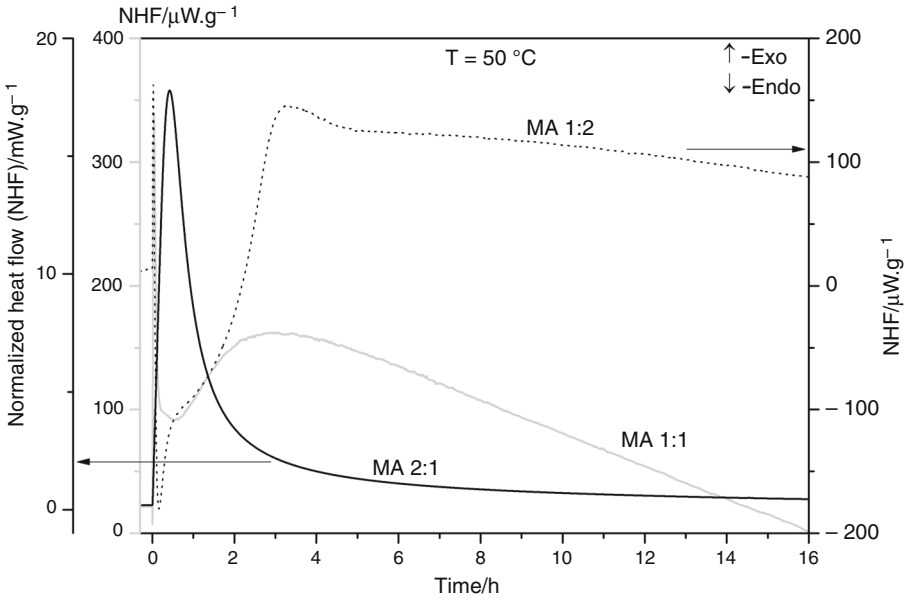

Fig. 10 Heat flow curves of reactive magnesia–hydratable alumina pastes hydrated at 50 °C for w/s = 0.7, normalized to mass of dry mixtures (with in situ mixing). MgO/Al_2O_3 molar ratio (M/A for short) of 1:1, 2:1 and 1:2

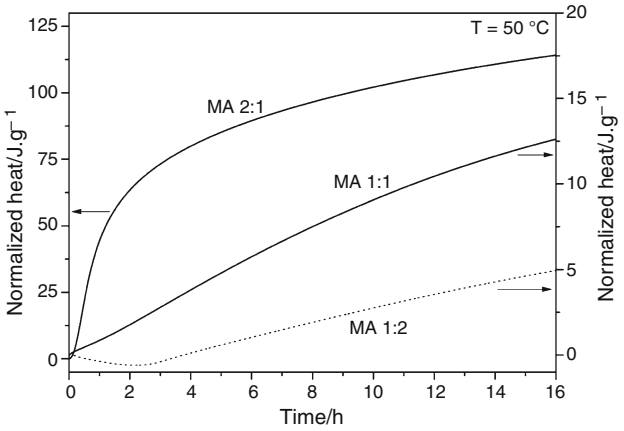

Fig. 11 Cumulative heat of reactive magnesia–hydratable alumina pastes hydrated at 50 °C for w/s = 0.7. MgO/Al_2O_3 molar ratio (M/A for short) of 1:1, 2:1 and 1:2

liquid and $Mg(OH)_2$ formation. Depending on the composition of the sample, a decrease in the first peak intensity associated with the increase in the MgO content is clearly observed (Fig. 8b). Within a few hours, second exotherm appears in the MA 1:2 sample (Fig. 8a). Such peak is mostly associated with the primary reaction in which anhydrous solids are converted to the product phases, i.e., the further formation of $Mg(OH)_2$, and both AH_3-gel and amorphous M–A–H phase. The times at which these reaction peaks occur and their durations exhibit a strong MgO/Al_2O_3 molar ratio dependence. For example, this second exothermic peak was split into two heat effects, as it can be observed in the MA 1:1 and MA 2:1 curves (Fig. 8a). The third MgO/Al_2O_3 molar ratio-dependent feature is the appearance of periods of low heat evolution

Table 6 The total amount of heat released during hydration of binders at 16 *h* of curing time in J g^{-1} exposed to 25 °C and 50 °C isothermal temperatures

Samples	T = 25/°C	T = 50/°C
MA 1:1	24	13
MA 2:1	54	114
MA 1:2	12	5

between the mixing and reaction peaks. This induction period which is generally a time of minimal hydration activity between the initial hydration reactions upon wetting and the later primary reaction both MgO and Al_2O_3 with water to form $Mg(OH)_2$, AH_3-gel and amorphous M–A–H phase occurs between about 20 min and < 2 h (MA 2:1), 2 h (MA 1:1) or 4 h (MA 1:2). Thus, for a higher MgO content, the accelerated hydration peak is intensified and it appears earlier (Fig. 8a). Figure 9 shows curves of the total heat liberated during the first 72 h of reaction of MA 2:1, MA 1:1 and MA 1:2 mixtures. Comparing the three data, it can be seen clearly that the extent of heat liberation increases with increasing MgO content in the hydrating pastes. The slope of the heat liberation curve of MA 2:1 sample exhibits period of rapid reaction, followed by extended periods of slow reaction. This behavior is consistent with a hydration mechanism which is initially controlled by interfacial reactions between water molecules and the solid surfaces, and then controlled by diffusion processes. Hydration at higher temperature, i.e., 50 °C, brings about a reduction in the total amount of heat released during hydration of the MA 1:1 and MA 1:2 pastes in the first 16 h (Fig. 11 and Table 6). The reason for this is

Table 7 Calorimetric data for the $MgO–Al_2O_3$ cementitious matrices cured at 25 °C and 50 °C

Samples	Intensity of the first wetting exothermic peak	Induction period
T = 25 °C		
MA 1:1	1.8 mW g^{-1}	20 min–2 h
MA 21	2.4 mW g^{-1}	20 min– < 2 h
MA 12	1.7 mW g^{-1}	20 min–4 h
T = 50 °C		
MA 11	460 μW g^{-1}	No
MA 21	18 mW g^{-1}	No
MA 12	Endothermic effect	No

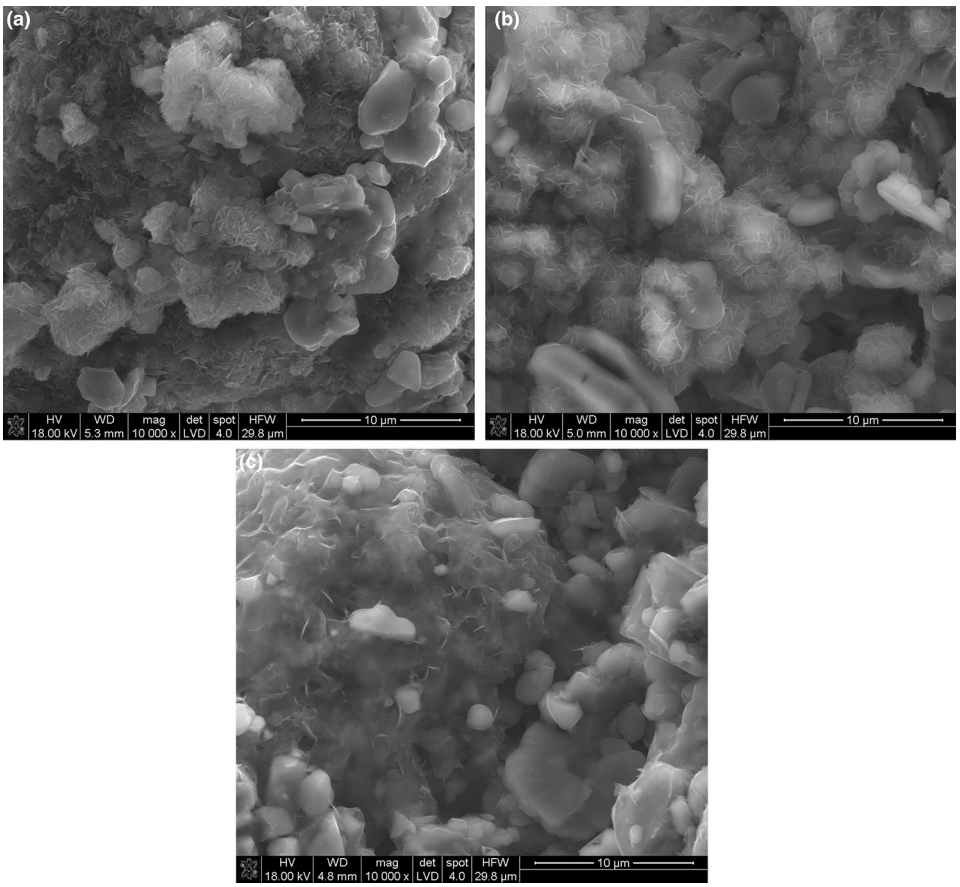

Fig. 12 Morphologies of hydrated MAH pastes with different MgO/Al_2O_3 molar ratio prepared at w/s = 0.7 and cured for 50 days at 50 °C: **a** MA 1:1, **b** MA 2:1, **c** MA 1:2

evidently the inability to achieve complete hydration at elevated temperature since the hydration products adhere firmly to the surfaces of the anhydrous reactive alumina. However, the sample prepared with an excess of MgO (MA 2:1) with respect to the stoichiometric value of MA 1:1 exhibits an increase in the total heat evolved in the first 16 h because the temperature activates hydration process of MgO. Moreover, the induction period is absent and both mixing and reaction peaks overlap in the calorimetric curve of the MA 2:1 sample at temperature of 50 °C (Table 7). It may be also supposed that an endothermic valley presented in Fig. 10 for MA 1:2 sample corresponds to the dissolution/hydrolysis of alumina and the exothermic peak is related to the dissolution of magnesia and the formation of hydration products. As can be seen in Fig. 10, an accelerated hydration peak occurs in the MA 1:1 paste when hydration is carried out at 50 °C.

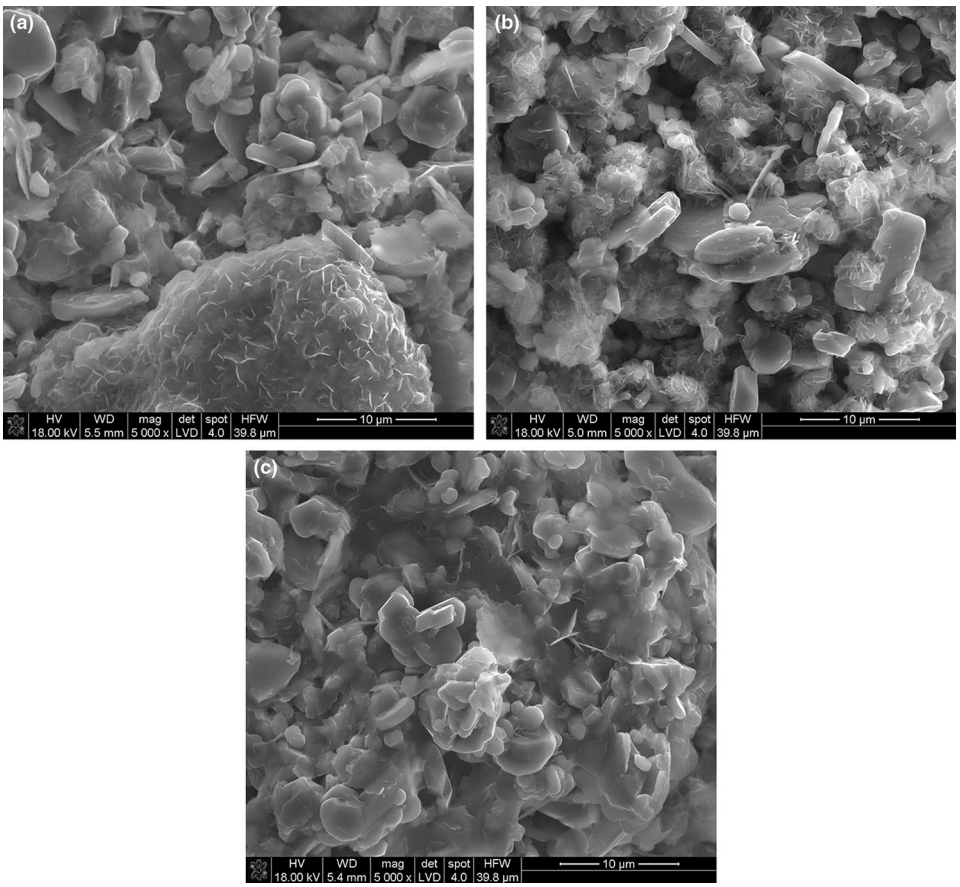

Fig. 13 Morphologies of hydrated MAH pastes with different MgO/Al_2O_3 molar ratio prepared at w/s = 0.7 and cured for 259 days at 50 °C: **a** MA 1:1, **b** MA 2:1, **c** MA 1:2

Morphological structure of Mg–Al cementitious matrices: SEM and TEM analysis

The MgO/Al_2O_3 molar ratio influences both the hydration behavior of magnesia–alumina-based binder systems, as previously highlighted in XRD, DSC–TG–EGA and microcalorimetry discussion. The morphological changes of samples due to time were also studied by SEM method. Figure 12a–c presents SEM micrographs of the neat MA pastes with MgO/Al_2O_3 molar ratios of 1:1, 2:1 and 1:2, respectively, prepared with 0.7 of w/s and cured at 50 °C for 50 days. Besides, Fig. 13a–c presents SEM images of these hydrated materials subjected to 259 days of curing period. This curing time-dependent morphological changes of Mg–Al cementitious matrices are evident from the micrographs in Figs. 12 and 13. SEM image of the fracture surface of the paste prepared with an excess of Al_2O_3 (MA 1:2, Fig. 12c) with respect to the stoichiometric value of MA 1:1 (Fig. 12a) exhibits dense structure of amorphous or semicrystalline gel of M–A–H phase and $Mg(OH)_2$ that covers the surface of the reactive alumina grains. A few crystals of $Mg(OH)_2$ are present in spongy clusters of 50-day cured samples (Fig. 12a, b) between Al_2O_3 particles. As time proceeded to 259 days, most of these crystals disappeared; thus, it seems that $Mg(OH)_2$ was consumed. SEM images provide excellent evidence of the existence of hexagonal-shape sheet of hydrotalcite-like crystals formed during hydration process of the mixture of MgO and Al_2O_3 micro-powders. These Mg-, Al-containing crystals are embedded in the investigated 50-day hydrated cementitious matrices between alumina/hydrated alumina and magnesium hydroxide particles (Fig. 12a–c). A greater amount of hydration products, i.e., newly formed thin-walled plates of MAH compound, appeared in the 259-day cured material (Fig. 13a–c). These thin-walled crystals are embedded in the coagulated products of the 259-day cured MA cementitious pastes.

Conclusions

In this paper, an experimental investigation of hydration mechanism of the binary cementitious pastes containing MgO and Al_2O_3 micro-powders was presented. According

to the current research, some certain conclusions can be drawn:

1. The MgO/Al_2O_3 molar ratio affects the heat flow curves of reactive magnesia-hydratable alumina pastes hydrated at 25 and 50 °C.
2. Structural changes in the hardened binary cementitious pastes containing MgO and Al_2O_3 micro-powders, subjected to the different time/temperature curing conditions, were studied at micrometer and nanometer levels.
3. Both MgO/Al_2O_3 molar ratio and curing time affect the substitution of Mg^{2+} ions by the Al^{3+} ions in brucite-like layers [$Mg(OH)_2$] of the binary cementitious pastes containing reactive MgO and Al_2O_3 micro-powders. Hence, an excess concentration of aluminum ions over the concentration of magnesium ions and prolonging the hardening time up to 2 years promote the formation of hydrotalcite-like hydration product.
4. The products formed are a Mg–Al–CO_3 hydrotalcite-like compound known as a Mg–Al layered double hydroxide (Mg–Al–LDH) and magnesium hydroxide.
5. The sharpening of Mg–Al–CO_3 hydrotalcite-like compound main peaks intensity means that the crystallinity and phase content of nanoscale Mg–Al–CO_3 hydrotalcite are effectively improved after the prolonged curing time.
6. The thermal stability of hydroxyls in hydration products can be placed in the decreasing order as follows: (Mg2Al)–OH hydrotalcite group > (Mg3)–OH-brucite group > (Mg3)–OH-hydrotalcite group.

Open Access This article is distributed under the terms of the Creative Commons Attribution 4.0 International License (http://creativecommons.org/licenses/by/4.0/), which permits unrestricted use, distribution, and reproduction in any medium, provided you give appropriate credit to the original author(s) and the source, provide a link to the Creative Commons license, and indicate if changes were made.

Funding This study was funded by The National Centre for Research and Development (Poland) within the framework of LIDER VIII Project No. LIDER/5/0034/L-8/16/NCBR/2017.

References

1. Zhang Y, Li Y, Dai Y, Liu J, Xu Y. Hydration evolution of MgO–SiO_2 slurries in the presence of sodium metasilicate. Ceram Int. 2018;44:6626–33.
2. Nied D, Enemark-Rasmussen K, L'Hopital E, Skibsted J, Lothenbach B. Properties of magnesium silicate hydrates (M–S–H). Cem Concr Res. 2016;79:323–32.
3. Szczerba J, Prorok R, Śnieżek E, Madej D, Maślona K. Influence of time and temperature on ageing and phases synthesis in the MgO–SiO_2–H_2O system. Thermochim Acta. 2013;567:57–64.
4. Li Z, Yu Q, Chen X, Liu H, Zhang J, Zhang J, Yang Y, Wei J. The role of MgO in the thermal behavior of MgO-silica fume pastes. J Therm Anal Calorim. 2017;127:1897–909.
5. Bai L, Ma Y, Zhao W, Deng Y, Li S. Optimization and mechanism in preparing active magnesium oxide from magnesite. J Therm Anal Calorim. 2017;129:1103–9.
6. Liu B, Thomas PS, Ray AS, Guerbois JP. A TG analysis of the effect of calcination conditions on the properties of reactive magnesia. J Therm Anal Calorim. 2007;88:145–9.
7. Liu XW, Feng YL, Li HR, Zhang P, Wang P. Thermal decomposition kinetics of magnesite from thermogravimetric data. J Therm Anal Calorim. 2012;107:407–12.
8. Ren H, Chen Z, Wu Y, Yang M, Chen J, Hu H, Liu J. Thermal characterization and kinetic analysis of nesquehonite, hydromagnesite, and brucite, using TG-DTG and DSC techniques. J Therm Anal Calorim. 2014;115:1949–60.
9. Sawków J, Nocuń-Wczelik W. Calorimetric studies of refractory corundum Calcium aluminate composites. J Therm Anal Calorim. 2003;74:451–8.
10. Ye G, Troczynski T. Effect of magnesia on strength of hydratable alumina-bonded castable refractories. J Mater Sci. 2005;40:3921–6.
11. Ma W, Brown PW. Mechanisms of reaction of hydratable aluminas. J Am Ceram Soc. 1999;82:453–6.
12. Santos T Jr, Pinola FG, Luz AP, Pagliosa C, Pandolfelli VC. Al_2O_3–MgO refractory castables with enhanced explosion resistance due to in situ formation of phases with lamellar structure. Ceram Int. 2018. https://doi.org/10.1016/j.ceramint.2018.01.246.
13. Sako EY, Braulio MAL, Brant PO, Pandolfelli VC. The impact of pre-formed and in situ spinel formation on the physical properties of cement-bonded high alumina refractory castables. Ceram Int. 2010;36:2079–85.
14. Braulio MAL, Rigaud M, Buhr A, Parr C, Pandolfelli VC. Spinel-containing alumina-based refractory castables. Ceram Int. 2011;37:1705–24.
15. Madej D. Size-dependent hydration mechanism and kinetics for reactive MgO and Al_2O_3 powders with respect to the calcia-free hydraulic binder systems designed for refractory castables. J Mater Sci. 2017;52:7578–90.
16. Madej D, Ortmann Ch, Szczerba J, Jacewicz M. Calorimetry and other methods in the studies of reactive magnesia-hydratable alumina-microsilica hydrating mixtures. J Therm Anal Calorim. 2016;126:1133–42.
17. Sharma U, Tyagi B, Jasra RV. Synthesis and characterization of Mg–Al–CO_3 layered double hydroxide for CO_2 adsorption. Ind Eng Chem Res. 2008;47:9588–95.
18. Stanimirova T, Hibino T, Balek V. Thermal behavior of Mg–Al–CO_3 layered double hydroxide characterized by emanation thermal analysis. J Therm Anal Calorim. 2006;84:473–8.
19. Mills SJ, Christy AG, Génin J-MR, Kameda T, Colombo F. Nomenclature of the hydrotalcite supergroup: natural layered double hydroxides. Mineral Mag. 2012;76:1289–336.
20. Zadaviciute S, Baltakys K, Bankauskaite A. The effect of microwave and hydrothermal treatments on the properties of hydrotalcite. J Therm Anal Calorim. 2017;127:189–96.
21. Smoláková L, Frolich K, Troppová I, Kutálek P, Kroft E, Čapek L. Determination of basic sites in Mg–Al mixed oxides by combination of TPD-CO_2 and CO_2 adsorption calorimetry. J Therm Anal Calorim. 2017;127:1921–9.
22. ICDD and ICSD PDF-2 database products.
23. Lin YJ, Li DQ, Evans DG, Duan X. Modulating effect of Mg–Al–CO_3 layered double hydroxides on the thermal stability of PVC resin. Polym Degrad Stab. 2005;88:286–93.
24. Wang Y, Luo S, Wang Z, Fu Y. Structural and textural evolution of nanocrystalline Mg–Al layered double hydroxides during mechanical treatment. Appl Clay Sci. 2013;80–81:334–9.

25. Zhou J, Su Y, Zhang J, Xu X, Zhao J, Qian G, Xu Y. Distribution of OH bond to metal-oxide in $Mg_{3-x}Ca_xFe$layered double hydroxide (x = 0–1.5): its role in adsorption of selenate and chromate. Chem. Eng J. 2015;262:383–9.
26. Stanimirova T, Balek V. Characterization of layered double hydroxide Mg–Al–CO_3 prepared by re-hydration of Mg–Al mixed oxide. J Therm Anal Calorim. 2008;94:477–81.
27. Ookubo A, Ooi K, Tani F, Hayashi H. Phase transition of Cl–intercalated hydrotalcite-like compound during ion exchange with phosphates. Langmuir. 1994;10:407–11.
28. Zhang J, Xu YF, Qian G, Xu ZP, Chen C, Liu Q. Reinvestigation of dehydration and dehydroxylation of hydrotalcite-like compounds through combined TG-DTA-MS analyses. J Phys Chem C. 2010;114:10768–74.